

Experimental study of the compensation method for atmospheric attenuation of probing laser radiation in active electro-optical systems that provide an increase of target image contrast

L.F. Kupchenko, A.S. Rybiak, O.A. Goorin, A.P. Hurin, A.V. Ponomar, O.V. Biesova

Ivan Kozhedub Kharkiv National Air Force University
77/79, Sumska str., 61023 Kharkiv, Ukraine
Corresponding author e-mail: anattoliy@meta.ua

Abstract. The article deals with the experimental study of the compensation method for atmospheric attenuation of laser radiation in active electro-optical remote sensing systems with dynamic spectral processing of optical signals that provides an increase of target image contrast. The compensation method for atmospheric attenuation of laser radiation in active electro-optical systems consists in forming the spectral intensity of the probing radiation not only on the basis of *a priori* data on the spectral features of the reflecting surfaces of the target and the background, but also taking into account the spectral transmittance of the optical radiation propagation medium. The experimental setup has been developed, in which the source of radiation in the transmitting part of the electro-optical system is three semiconductor lasers operating in the ranges of the red, green and blue parts of the spectrum. Absorption light filters were used in the experiment as elements simulating the spectral properties of the reflecting surfaces of the target and background. The cuvettes with a liquid absorbing optical radiation were used as elements simulating atmospheric attenuation.

Keywords: active electro-optical system, dynamic spectral processing, atmospheric attenuation of radiation, semiconductor lasers.

<https://doi.org/10.15407/spqeo26.01.105>
PACS 42.55.-f, 42.79.-e

Manuscript received 21.11.22; revised version received 19.01.23; accepted for publication 08.03.23; published online 24.03.23.

1. Introduction

All electro-optical systems according to the principle of formation of information fields (radiation fields) can be separated into passive and active ones. Passive electro-optical systems use information fields formed by natural radiation in the object space. The active method of constructing electro-optical systems involves creation of an information field by using external radiation sources.

In the work devoted to multispectral electro-optical systems, the advantages of active electro-optical systems (AEOS) over the passive ones are formulated in [1]. It is noted that in passive electro-optical systems the radiance for radiation reflected from target depends on the imaging scheme, in particular, on the mutual spatial position of the Sun, target and receiving system. Therefore, when using the passive electro-optical systems, errors occur when comparing the current spectral features with the reference ones. Active electro-optical imaging systems can partially eliminate the disadvantages of passive electro-optical systems, since the radiation source and receiver have fixed positions during formation of the information field.

Our analysis of literature sources has shown that the development of laser radiation sources with a wide range of technical characteristics contributes to the intensive development of AEOS [2]. Also, the studies related to the development of spectral imaging systems with active illumination are of considerable practical interest [3–11].

Developing research in this area, in [1] the authors outlined the principles for constructing active electro-optical detection systems with dynamic spectral processing of optical signals. In such systems, the received signal is processed in the pre-detector region that is in the optical range, and the spectral composition of the probing radiation is formed using multispectral laser signals based on *a priori* information about the spectral reflectances of the target and background. The probing signal formed in this way enables to suppress the background signal with minimal attenuation of the target signal, which results in an increase of the image contrast at the output of AEOS.

However, when propagating in air the probing signal is exposed to atmospheric interference, which leads to a change in its spectral intensity, and, as a result, to a

decrease in the efficiency of signal processing by AEOS. In [12], the method was developed, which enables to compensate the atmospheric attenuation of laser radiation, when using the AEOS. The method is based on the fact that the spectral intensity of the probing radiation is formed not only on the basis of preliminary data on the spectral reflectances of the target and background, but also with account of the *a priori* known spectral transmittance of the propagation medium for a multispectral optical signal.

The purpose of this paper is to experimentally test the previously developed compensation method for atmospheric attenuation of laser radiation in AEOS with dynamic spectral processing of optical signals in order to increase the contrast of target images.

2. Dynamic spectral processing of optical radiation in an active electro-optical system

The physical basis for the construction of AEOS with pre-detector spectral processing is the fact that colored surfaces have a selective ability to reflect and absorb light of various wavelengths. If the surface is capable of reflecting red rays, then when it's illuminated with green rays, the surface will reflect an insignificant part of the radiation energy and will be dark in the image [13].

The fundamentals of dynamic spectral processing of optical radiation in AEOS are described in [1]. It is shown that for their implementation, the surface studied must be illuminated by a radiation source, in which the spectral radiance $L_{\Sigma e}(\lambda)$ is a weighted sum of the spectral radiances $L_{ek}(\lambda)$ of monochromatic emitters:

$$L_{\Sigma e}(\lambda) = \sum_{k=1}^m L_{ek}(\lambda) = \sum_{k=1}^m A_k \varphi_{ek}(\lambda), \quad (1)$$

where A_k is the weight coefficient of the spectral radiance of the k -th radiation source; $\varphi_{ek}(\lambda)$ is the spectral radiance of the k -th source at $A_k = 1$.

Then the optical signal arriving at the radiation receiver of AEOS is determined by the dot product of the vector $\vec{F} = [f_1, K, f_k, K, f_m]^T$ of its instrumental function and the vector $\vec{X} = [x_1, K, x_k, K, x_m]^T$ of the input optical signal representing the spectral properties of the reflecting surface [1]:

$$\Phi_e = q \sum_{k=1}^m f_k x'_k = \vec{F}^T \vec{X}, \quad (2)$$

where x'_k is the relative radiation flux arriving at the input of the receiver of AEOS for the k -th monochromatic component of the radiation source; f_k is the coordinate of the vector \vec{F} of the instrumental function of AEOS, which is the weighted value of the spectral radiance of the k -th monochromatic component of the radiation source of AEOS $f_k = A_k$.

The vector \vec{X} coordinates correspond to the fluxes of radiation entering the input of the AEOS receiver for each monochromatic component of the radiation source [1]:

$$x_k = q x'_k = q \int_{\lambda_{\min}}^{\lambda_{\max}} \varphi_{ek}(\lambda) \tau_{o1}(\lambda) \tau_a^2(\lambda) \rho(\lambda) \tau_{o2}(\lambda) d\lambda, \quad (3)$$

where $q = \frac{\pi D_{out}^2 S_{rr}}{16z^2} \left(\frac{D_{in}}{f'} \right)^2$ is a parameter that depends

on the distance to the probed surface z and design parameters of AEOS (D_{out} is the diameter of the exit pupil of the optical subsystem of the radiation source; D_{in}, f' is the diameter of the entrance pupil and the focal length of the optical subsystem of the receiving channel in AEOS; S_{rr} is the area of the radiation receiver) [5, 6]; $\tau_a(\lambda)$ is the spectral transmittance of the medium; $\tau_{o1}(\lambda), \tau_{o2}(\lambda)$ are the spectral transmittances of the optical systems of the transmitting and receiving channels in AEOS; $\rho(\lambda)$ is the spectral reflectance of the probed surface (for diffuse reflection); $\lambda_{\min} K \lambda_{\max}$ is the operating wavelength range inherent to AEOS.

To implement dynamic spectral processing of optical radiation, AEOS (Fig. 1) should include a controlled laser radiation source (LRS), a receiving optical subsystem (ROS), and a radiation receiver (RR). The source of laser radiation consists of m sources operating in different wavelength ranges. This provides independent control of the intensity proper to each of them.

At the output of the radiation receiver of this AEOS, the signal Y proportional to (and ideally equal to) the dot product of the vector of its instrumental function \vec{F} and the vector of the input optical signal \vec{X} containing information about the spectral properties of the reflecting surface will be measured. If the radiation receiver is characterized by spectral sensitivity $r(\lambda)$, then, with account of (2) and (3), the expression for the signal at the output of AEOS will take the following form

$$Y = q \sum_{k=1}^m f_k \int_{\lambda_{\min}}^{\lambda_{\max}} \varphi_{ek}(\lambda) \tau_{o1}(\lambda) \tau_a^2(\lambda) \rho(\lambda) \tau_{o2}(\lambda) r(\lambda) d\lambda. \quad (4)$$

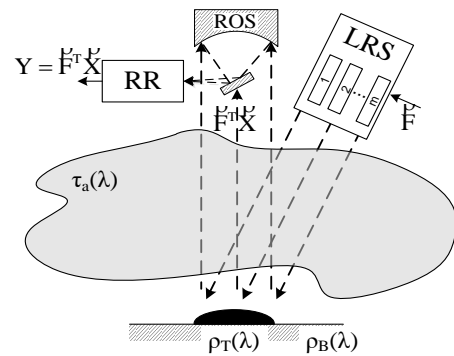


Fig. 1. Scheme of the active electro-optical system with dynamic spectral processing of optical radiation.

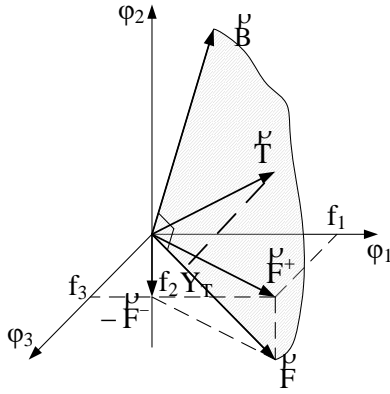


Fig. 2. Vector representation of dynamic spectral processing of optical radiation in AEOS orders to increasing the contrast of the target image.

Thus, the mathematical basis of dynamic spectral processing of optical signals is their vector representation. The optical radiation of the target and the background in this case is represented as the vectors \vec{T} and \vec{B} in a multidimensional spectral space $\{\varphi_1, \varphi_2, \varphi_3, K\}$ (Fig. 2) [12].

It is known [1, 11, 12] that through the use of dynamic spectral processing of optical radiation an increase in the image contrast of the target C is provided by reducing the background signal Y_B at the output of AOES with minimal attenuation of the output signal of the target Y_T . The image contrast of the observed object (target) at the output of AEOS with dynamic spectral processing is determined as follows:

$$C = \frac{Y_T - Y_B}{Y_T + Y_B}, \quad (5)$$

where Y_T and Y_B are the signals of the target and background at the output of AEOS.

To increase the contrast of the target image, the filter vector \vec{F} must be perpendicular to the background vector \vec{B} and lie in a plane that passes through the target \vec{T} and background \vec{B} vectors. In this case, background spectral components will be suppressed due to the fact that the dot product $\vec{F}^T \vec{B}$ will be equal to zero. The filter vector \vec{F} in this case is calculated as based on *a priori* information about the spectral features of the target and background by using the following expression [12]:

$$\vec{F} = r(\vec{T} - N \cdot \vec{B}), \quad (6)$$

where $N = \vec{T}^T \vec{B} / \vec{B}^T \vec{B}$ is the projection of target vector \vec{T} onto the unit vector $\vec{B}^o = \vec{B} / \sqrt{\vec{B}^T \vec{B}}$ of the background vector normalized to its length $\|\vec{B}\| = \sqrt{\vec{B}^T \vec{B}}$; r is the normalizing multiplier that ensures maximization of the optical signal received by the radiation detector:

$$r = 1 / \max_k (t_k - N \cdot b_k), \quad (7)$$

where t_k and b_k are the coordinates of the target and background vectors, respectively.

In three-dimensional space, Fig. 2 shows the arrangement of vectors during dynamic spectral processing, and the magnitude of the projections for each of the vectors reflects the value of the radiation intensity for a certain wavelength. It is shown that the filter vector $\vec{F} = f_1 \varphi_1 - f_2 \varphi_2 + f_3 \varphi_3$ and the background vector $\vec{B} = b_1 \varphi_1 + b_2 \varphi_2 + b_3 \varphi_3$ are orthogonal, and the vector representing the spectral properties of the target $\vec{T} = t_1 \varphi_1 + t_2 \varphi_2 + t_3 \varphi_3$ lies in the plane passing through the vectors \vec{B} and \vec{F} .

Thus, using the vector representation of the optical signals of the target and the background, the instrumental function of AEOS is determined, which provides an increase of the contrast of the target image. It is shown that the vector of the instrumental function of AEOS must be orthogonal to the background vector and lie in the plane passing through the target and background vectors.

3. Influence of atmospheric interferences on the operation of AEOS with dynamic spectral signal processing

In AEOS with dynamic spectral processing, the spectral composition of the probing radiation is formed as a sum of laser signals, the intensities of which are calculated on the basis of *a priori* information about the spectral reflectance of the target and background. However, when propagating the probing signal is exposed to atmospheric interference, which leads to a change in its spectral intensity and, as a result, to a decrease in the efficiency of image processing.

The attenuation and distortion of optical signals in the atmosphere is due to two main processes [14, 15]:

- absorption of radiation by gaseous components;
- molecular and aerosol attenuation (scattering) of radiation.

Absorption of radiation is caused by the presence of various gases in the atmosphere and has a pronounced selective character.

In the general case, the process of attenuation of optical radiation in the atmosphere can be described by the following expressions:

- spectral extinction coefficient of the atmosphere – $\varepsilon(\lambda)$;
- spectral transmittance of the atmosphere – $\tau_a(\lambda)$.

With a single scattering of radiation in a homogeneous medium along the propagation path, its spectral transmittance is described by the Beer–Lambert–Bouguer law and is defined by the following expression [15]:

$$\tau_a(\lambda) = I(\lambda) / I_0(\lambda) = \exp[-\varepsilon(\lambda) \cdot l], \quad (8)$$

where $I(\lambda)$ is the spectral intensity of the radiation that has passed the distance l ; $I_0(\lambda)$ is the spectral intensity of radiation at the beginning of the path.

To determine the extinction coefficient of the atmosphere, we use the Koschmieder expression [15], which establishes the relationship between the extinction coefficient of the atmosphere $\varepsilon_{0.55}$ at the wavelength $0.55 \mu\text{m}$ and the meteorological optical range (meteorological range) R_{vis} . The meteorological optical range is the distance at which the contrast between a certain type of source (test object) $C_0 = 1$ and the surrounding background is reduced to the threshold of the contrast sensitivity of the eye $C_T = 0.05$ (in accordance with the requirements of the International Committee on illumination [16]):

$$R_{vis} = \frac{1}{\varepsilon_{0.55}} \ln \left(\frac{C_0}{C_T} \right) = \frac{3}{\varepsilon_{0.55}}. \quad (9)$$

The calculation of the spectral extinction coefficient in the wavelength range of $0.4 \dots 3 \mu\text{m}$ is performed using the following formula [15]:

$$\varepsilon(\lambda) = \frac{3}{R_{vis}} \left(\frac{0.55}{\lambda} \right)^{0.585 R_{vis}^{1/3}}, \quad (10)$$

where the meteorological optical range R_{vis} is expressed in kilometers and the wavelength λ is expressed in micrometers.

It should be taken into account that in AEOS, when calculating the effect of atmosphere, attenuation in two sections should be taken into account: propagation in the path from the source to the probing surface, and then from the surface to the receiving device:

$$\tau_a^2(\lambda) = \exp[-2 \cdot \varepsilon(\lambda) \cdot z], \quad (11)$$

where $z = l/2$ is the range to the surface, which is irradiated by AEOS.

Analysis of expressions (10) and (11) showed that the value of the spectral transmittance squared of the atmosphere $\tau_a^2(\lambda)$ decreases with decreasing wavelength λ of optical radiation. In this case, with an increase in the range z to the probed surface, the difference in the values of the spectral transmittance for different wavelengths increases. Consequently, the squared spectral transmittance of the atmosphere $\tau_a^2(\lambda)$ depends both on the wavelength λ of the optical radiation and on the range z to the probed surface.

4. Compensation method for atmospheric attenuation of radiation in AEOS with dynamic spectral processing

The method for compensation of the atmospheric attenuation of laser radiation in AEOS is described in [12]. The method is based on the fact that the spectral intensity of the probing radiation is formed not only using *a priori* information about the spectral reflectances of the target and the background, but also taking into account the preliminary known spectral transmittance of the propagation medium for a multispectral optical signal.

The method providing compensation of atmospheric attenuation of laser radiation includes the following steps:

1) the vector of the instrumental function of AEOS $\overset{P}{F} = [f_1, K, f_k, K, f_m]^T$ (where m is the number of monochromatic emitters) is calculated, which provides an increase in contrast (5) for the case when there is absence of radiation attenuation by the propagation medium $\tau_a^2(\lambda) = 1$;

2) the normalized correction vector $\overset{P}{F}_{corr n} = [f_1^{corr n}, K, f_k^{corr n}, K, f_m^{corr n}]^T$ is calculated, the coordinates of which are defined as follows [12]:

$$f_k^{corr n} = K_n \cdot \frac{f_k}{\tau_{ak}^2} = \frac{\tau_{a \min}^2}{f_{\min}} \cdot \frac{f_k}{\tau_{ak}^2}, \quad (12)$$

where $K_n = \min_k \left(\tau_{ak}^2 / f_k \right) = \tau_{a \min}^2 / f_{\min}$ is the normalizing factor; $\tau_{a \min}^2$ and f_{\min} are the square of the transmittance of the propagation medium and the coordinate of the vector $\overset{P}{F}$ (calculated at the first stage), the ratio of which is minimal;

3) dynamic spectral processing of optical radiation is carried out by calculating the radiation flux at the receiver input after correction, which is the dot product of the input signal vector $\overset{P}{X}$ with a normalized correction vector $\overset{P}{F}_{corr n}$:

$$\Phi_{e \text{ corr}} = \overset{P}{F}_{corr n}^T \overset{P}{X}. \quad (13)$$

Thus, the radiation flux arriving at the radiation receiver of AEOS with atmospheric attenuation compensation is the dot product of the input signal vector with the correction vector. In this case, the correction vector is formed on the basis of preliminary information about the spectral intensity of the probing radiation, the spectral transmittance of the atmosphere, as well as the spectral reflection coefficients of the target and background.

5. Composition and scheme of the experimental setup

For the verification of the developed method for compensating the atmospheric attenuation of laser radiation in AEOS with dynamic spectral processing, an experimental setup was developed, the block diagram of which is shown in Fig. 3. When developing the experimental setup, the results presented in [17] were used.

The experimental setup included the following blocks and elements:

- transmitting and receiving blocks;
- elements simulating target and background signals;
- elements simulating the absorbing properties of the atmosphere.

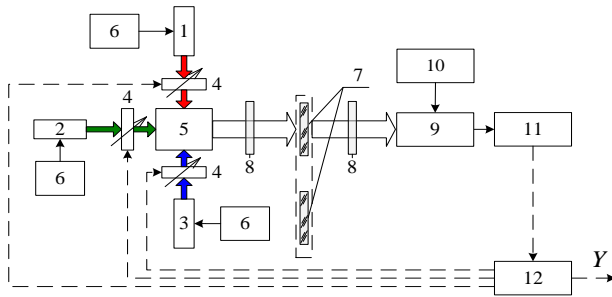


Fig. 3. Block diagram of the experimental setup.

The transmitting unit of the experimental setup consisted of the following devices:

- semiconductor laser 1 with the wavelength of radiation $\lambda = 635$ nm;
- semiconductor laser 2 with the wavelength of radiation $\lambda = 532$ nm;
- semiconductor laser 3 with the wavelength of radiation $\lambda = 450$ nm;
- three attenuators 4, providing control of the laser radiation intensity;
- dichroic prism 5 for spatial alignment of laser radiation into one beam;
- three power supplies 6 for lasers.

The receiving unit of the experimental setup included the following devices:

- photomultiplier 9 with the power supply 10;
- microammeter 11;
- computer 12.

Elements that imitate the optical signals of the target and the background and the absorption properties of the atmosphere, in Fig.3 are labeled 7 and 8, respectively. The elements simulating the optical signals of the target and the background were two sets of absorption light filters. In the first set, the filters simulating the optical signals of the target (GG-1) and the background (YGG-6) had approximately the same spectral transmittance. Light filters of the second set, simulating the signals of the target (BG-2) and the background (YGG-6), had spectral features that differed significantly.

The choice of light filters was carried out on the basis of the calculation of their spectral transmittances. The calculation was carried out using information on the absorption coefficients of light filters, induced in the catalog of colored glass [18]. When calculating the spectral transmittances, the reflection from the surface of the light filters was also taken into account.

To simulate the absorbing properties of the atmosphere on the “transmitter-target” and “target-receiver” paths, two identical cuvettes with a liquid absorbing radiation in the optical wavelength range of laser sources were used. A solution of milk with distilled water was used as a liquid. To do this, 0.06 g of milk diluted with distilled water in a ratio of 1:1 was added to 15 g of distilled water.

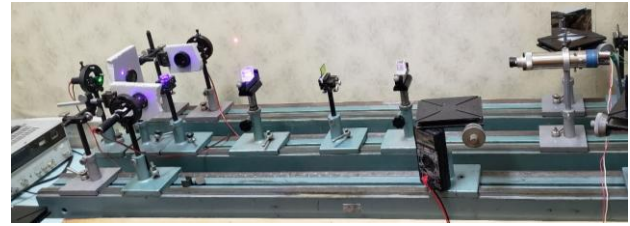


Fig. 4. General view of the experimental setup to study the method for attenuation compensation of laser radiation in AEOS.

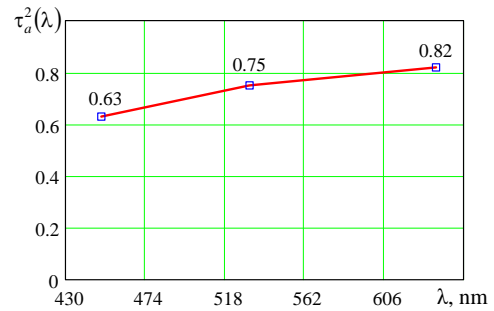


Fig. 5. Spectral transmittance squared of the cuvettes with radiation-absorbing liquid as a function of the laser radiation wavelength.

Fig. 4 shows a general view of the experimental setup for studying the method of compensating the attenuation of laser radiation in AEOS with dynamic spectral filtering.

Fig. 5 shows the dependence of the experimentally obtained spectral transmittance squared of cuvettes with radiation-absorbing liquid on the wavelength of laser radiation.

6. Experimental technique

The procedure for carrying out the experiment to study the method of compensating atmospheric attenuation of laser radiation in AEOS with dynamic spectral processing consisted of three successive stages.

Stage 1. Dynamic spectral processing in the interests of increasing contrast in the absence of attenuation of laser radiation.

At this stage, an experimental study of the process of dynamic spectral processing of optical radiation was carried out in order to increase the contrast of the target image at the output of AEOS in the absence of attenuation by the propagation medium. When performing this research, the spectral features of filters simulating the optical signals of the target and background were measured first. To do this, three lasers of the transmitting unit of the experimental setup were turned on and the signals at the output of PMT were measured, first for the filter that simulates the target signal, and then for the filter simulating the background signal. Based on the obtained measurements in three-dimensional space, the

target vector $\overset{P}{T} = [t_B, t_G, t_R]^T$ and the background vector $\overset{P}{B} = [b_B, b_G, b_R]^T$ were formed. The coordinates of each of the vectors were the values of the current at the PMT output, when the corresponding laser was turned on.

Using the expressions (6), (7), as well as the measured vectors $\overset{P}{T}$ and $\overset{P}{B}$, the instrumental function vector $\overset{P}{F} = [f_B, f_G, f_R]^T$ was calculated, which provided an increase in the contrast of the target image at the output of AEOS.

Next, to implement optical spectral processing, vectors $\overset{P}{F}^+$ and $\overset{P}{F}^-$ were formed, and dynamic spectral processing of optical radiation was performed. To do this, the attenuators were used to set the radiation intensity of each laser included in the transmitting unit. First, the transmittances of the attenuators were adjusted in accordance with the coordinates of the vector $\overset{P}{F}^+$ (Fig. 2), and the radiation of the target and background $Y_T^+ = \overset{P}{F}^{+T} \overset{P}{T}$, $Y_B^+ = \overset{P}{F}^{+T} \overset{P}{B}$, respectively, was measured. And then, similar operations were performed for the vector $\overset{P}{F}^-$, and signals $Y_T^- = \overset{P}{F}^{-T} \overset{P}{T}$, $Y_B^- = \overset{P}{F}^{-T} \overset{P}{B}$ were measured.

After that, the target Y_T and background Y_B signals at the output of AEOS were calculated by subtracting the corresponding values that were measured for the vectors $\overset{P}{F}^+$ and $\overset{P}{F}^-$:

$$Y_T = \overset{P}{F}^{+T} \overset{P}{T} - \overset{P}{F}^{-T} \overset{P}{T}; \quad (14)$$

$$Y_B = \overset{P}{F}^{+T} \overset{P}{B} - \overset{P}{F}^{-T} \overset{P}{B}. \quad (15)$$

Using the expression (5), the contrast of target image at the output of AEOS was calculated. When calculating the contrast in the course of experimental studies, the following values were obtained: for the first pair of light filters (GG-1 – YGG-6) $C = 0.86$; for the second pair of filters (BG-2 – YGG-6) $C = 1$.

Stage 2. Dynamic spectral processing for increasing the contrast without compensating for the attenuation of laser radiation.

At this stage, there was made a study of the influence of the attenuation of laser radiation by the propagation medium on the contrast of the target image at the output of AEOS with dynamic spectral processing. To do this, cuvettes imitating the process of radiation passing through the atmosphere were installed on the

path of propagation of the probing radiation. In this case, the vector of the instrumental function of AEOS was not changed and remained the same as under ideal conditions (there is no atmospheric attenuation).

Next, dynamic spectral processing of the optical radiation was performed, the signals at the output of AEOS were measured, and the target contrast was determined by analogy with the previous stage.

When calculating the contrast at this stage of experimental studies, the following values were obtained: for the first pair of light filters (GG-1 – YGG-6) $C = 0.67$; for the second pair of filters (BG-2 – YGG-6) $C = 0.62$.

Stage 3. Dynamic spectral processing for increasing the contrast for the compensation of the attenuation of laser radiation.

At this stage, the process of compensating the attenuation of laser radiation by the propagation medium during dynamic spectral processing was studied. The attenuation compensation efficiency was evaluated by calculating the target image contrast and comparing it with the value obtained at the second stage.

To do this, first, using Eq. (12), the coordinates of the normalized correction vector were calculated with account of the spectral transmittance of the cuvettes simulating the properties of the atmosphere. Next, dynamic spectral processing of optical radiation was performed according to Eq. (13). To do this, using the attenuators, the laser radiation intensities were set using the current value at the PMT output in accordance with the coordinate values of the normalized correction vector.

The contrast values obtained in the course of experimental studies at this stage were: for the first pair of light filters (GG-1 – YGG-6) $C = 0.83$; for the second pair of filters (BG-2 – YGG-6) $C = 0.93$.

The contrast values for pairs of light filters (GG-1 – YGG-6) and (BG-2 – YGG-6), which were obtained during three stages of experimental studies of dynamic spectral processing of laser radiation, are shown in Table.

Thus, the results obtained in the course of experimental studies show that the developed method enables to compensate the attenuation of laser radiation by the atmosphere. This method provides an increase (as compared to the case without compensation) of the target contrast at the output of AEOS for a pair of GG-1 and YGG-6 light filters by 1.2 times, and for a pair of BG-2 and YGG-6 light filters – 1.5 times.

Table. Contrast values obtained in the course of experimental studies.

Contrast measurement condition	GG-1 and YGG-6	BG-2 and YGG-6
1. Target contrast in the absence of radiation attenuation by the atmosphere	0.86	1
2. Target contrast with attenuation of radiation by the atmosphere and without attenuation compensation	0.67	0.62
3. Target contrast in the presence of radiation attenuation by the atmosphere and using attenuation compensation	0.83	0.93

7. Conclusions

The results of experimental studies of a method for compensating atmospheric attenuation of laser radiation in AEOS with dynamic spectral processing of optical signals in order to increase the contrast of the target images have been presented. The scheme of an experimental setup for studying the method to compensate attenuation of laser radiation in AEOS has been developed. The transmitting part of the scheme included three semiconductor lasers operating in the ranges of the red, green and blue parts of the spectrum. Cuvettes with the liquid absorbing optical radiation were used as elements simulating atmospheric attenuation.

The possibility to compensate attenuation of multispectral laser radiation in an absorbing medium and to provide the increase of contrast inherent to the target image at the output of AEOS has been experimentally confirmed. The method of compensating for atmospheric attenuation of laser radiation in AEOS is based on the fact that the spectral intensity of the probed radiation is formed not only on the basis of preliminary data on the spectral features of the target and background, but also with account of the known in advance spectral transmittance of the medium.

Experimental studies included three stages. First, dynamic spectral processing of optical radiation was carried out in the absence of radiation attenuation in the atmosphere. Then, dynamic spectral processing of optical radiation was performed in the presence of radiation attenuation by the propagation medium and without its compensation. At the final stage, dynamic spectral processing of optical radiation was made in the presence of radiation attenuation by the propagation medium and with its compensation.

The efficiency of attenuation compensation has been evaluated by calculating the image contrast of the target at each stage of the study and comparing the obtained values. It has been experimentally ascertained that as a result of applying compensation for the attenuation of laser radiation, it is possible to increase (as compared to the case without compensation) the contrast value for a pair of light filters GG-1 – YGG-6 by 1.2 times, and for a pair of light filters BG-2 – YGG-6 – 1.5 times.

References

1. Kupchenko L.F., Karlov V.D., Rybiak A.S. *et al.* Active electro-optical system of targets detection with dynamic spectral processing of optical radiation. *SPQEO*. 2021. **24**, No 2. P. 218–226. <https://doi.org/10.15407/spqeo24.01.218>.
2. McManamon P.F. Review of ladar: A historic, yet emerging, sensor technology with rich phenomenology. *Opt. Eng.* 2012. **51**, No 6. P. 060901. <https://doi.org/10.1117/1.OE.51.6.060901>.
3. Steinvall O. Active spectral imaging and mapping. *Adv. Opt. Techn.* 2014. **3**, No 2. P. 161–178. <https://doi.org/10.1515/aot-2013-0064>.
4. Johnson B., Joseph R., Nischan M. *et al.* A compact, active hyperspectral imaging system for the detection of concealed targets. *Proc. SPIE*. 1999. **3710**, Detection and Remediation Technologies for Mines and Minelike Targets IV. <https://doi.org/10.1117/12.357002>.
5. Manninen A., Kääriäinen T., Parviainen T. *et al.* Long distance active hyperspectral sensing using high-power near-infrared supercontinuum light source. *Opt. Exp.* 2014. **22**, Issue 6. P. 7172–7177. <https://doi.org/10.1364/OE.22.007172>.
6. Liu Y., Tao Z., Zhang J. *et al.* Deep-learning-based active hyperspectral imaging classification method illuminated by the supercontinuum laser. *Appl. Sci.* 2020. **10**, No 9. P. 3088. <https://doi.org/10.3390/app10093088>.
7. Guo Z., Liu Y., Zheng X., Yin K. Active hyperspectral imaging with a supercontinuum laser source in the dark. *Chin. Phys. B*. 2019. **28**, No 3. P. 034206. <https://doi.org/10.1088/1674-1056/28/3/034206>.
8. Hempler N., Nicholls J., Malcolm G. Active hyperspectral sensing and imaging for remote spectroscopy applications. *Laser Focus World*. 2013. **49**, No 11. <https://www.laserfocusworld.com/test-measurement/spectroscopy/article/16556842/spectral-imaging-active-hyperspectral-sensing-and-imaging-for-remote-spectroscopy-applications>.
9. El Fakir C., Poffo L., Billiot B. *et al.* Active hyperspectral mid-infrared imaging on widely tunable QCL laser. *2019 21st Int. Conf. on Transparent Optical Networks (ICTON)*, Angers, France, 2019. P. 1–4. <https://doi.org/10.1109/ICTON.2019.8840448>.
10. El Fakir C., Hjejij M., Le Page R. *et al.* Active hyperspectral mid-infrared imaging based on a widely tunable quantum cascade laser for early detection of plant water stress. *Opt. Eng. SPIE*. 2021. **60**, No 2. P. 023106. <https://doi.org/10.1117/1.OE.60.2.023106>.
11. Kupchenko L.F., Goorin O.A., Karlov V.D. *et al.* Active electro-optical system with dynamic spectral processing of optical radiation. *2019 IEEE 8th Int. Conf. on Advanced Optoelectronics and Lasers (CAOL)*, Sozopol, Bulgaria, 2019. P. 489–492. <https://doi.org/10.1109/CAOL46282.2019.9019458>.
12. Kupchenko L.F., Rybiak A.S., Ponomar A.V. Compensation method for atmospheric attenuation of laser radiation in active electro-optical systems with dynamic spectral processing of optical signals. *Semiconductor Physics, Quantum Electronics and Optoelectronics*. 2022. **25**, No 2. P. 211–218. <https://doi.org/10.15407/spqeo25.02.211>.
13. Manolakis D., Marden D., Shaw G.A. Hyperspectral image processing for automatic target detection applications. *Lincoln Laboratory Journal*. 2003. **14**, No 1. P. 79–113.

14. Schott J.R. *Remote Sensing the Image Chain Approach*, 2nd ed. Oxford University Press, 2007.
15. Holst G.C. *Electro-Optical Imaging System Performance*, 6th ed. SPIE Press Book, 2017. <https://doi.org/10.1117/3.2588947>.
16. Christnacher F., Schertzer S., Metzger N. *et al.* Influence of gating and of the gate shape on the penetration capacity of range-gated active imaging in scattering environments. *Opt. Exp.* 2015. **23**, Issue 26. P. 32897–32908. <https://doi.org/10.1364/OE.23.032897>.
17. Kupchenko L.F., Rybiak A.S., Goorin O.A., Biesova O.V. Experimental researches of dynamic spectral processing of optical radiation in the active electro-optical system. *SPQEO*. 2022. **25**, No 1. P. 90–96. <https://doi.org/10.15407/spqeo25.01.090>.
18. *Colored Optical Glass and Special Glasses*. Catalogue, G.T. Petrovsky (Ed.). Dom optiki, Moscow, 1999.

Authors and CV



Leonid F. Kupchenko, Doctor of Technical Sciences, Professor, Senior Instructor at the Ivan Kozhedub Kharkiv National Air Force University, the author of more than 200 scientific publications including 1 monograph, 25 patents, 74 articles. The area of his scientific interests includes acousto-optics, optoelectronics, optimal processing of optical signals.

E-mail: kupch@meta.ua,
<https://orcid.org/0000-0002-8599-1944>



Anatolii S. Rybiak, PhD in Technical Sciences, Senior Researcher, Doctoral student at the Ivan Kozhedub Kharkiv National Air Force University, the author of more than 100 scientific publications including 2 monographs, 6 patents, 44 articles. The area of his scientific interests includes acousto-optics, optoelectronics, optimal processing of optical signals.

<https://orcid.org/0000-0002-7922-3690>



Oleg A. Goorin, PhD in Technical Sciences, Senior Instructor at the Ivan Kozhedub Kharkiv National Air Force University, the author of 22 scientific publications, 1 patent. The area of his scientific interests includes electro-optical systems, spectral filtration of optical signals, laser vision.

E-mail: goorin.oleg@gmail.com,
<https://orcid.org/0000-0002-7216-7497>



Artem P. Hurin, postgraduate student at the Ivan Kozhedub Kharkiv National Air Force University, the author of 3 scientific publications, 1 patent. The area of his scientific interests includes electro-optical systems, spectral filtration of optical signals, laser vision.

E-mail: tema0504@gmail.com,
<https://orcid.org/0000-0002-8536-4924>



Andriy V. Ponomar, Senior researcher at the Ivan Kozhedub Kharkiv National Air Force University, the author of 3 scientific publications. The area of his scientific interests includes electro-optical systems, spectral filtration of optical signals, laser vision.

E-mail: andreyponomar1980@gmail.com,
<https://orcid.org/0000-0001-6854-6892>



Oksana V. Biesova, PhD in Technical Sciences, Senior Researcher at the Ivan Kozhedub Kharkiv National Air Force University, the author of 30 scientific publications. The area of scientific interests includes radiolocation, optoelectronics, signal recognition.

E-mail: bytko75@ukr.net,
<https://orcid.org/0000-0001-7744-1339>

Authors' contributions

Kupchenko L.F.: conceptualization, project administration, writing – original draft (partially).

Rybiak A.S.: methodology, investigation, formal analysis, validation, writing – original draft, writing – review & editing, visualization.

Goorin O.A.: investigation, data curation.

Hurin A.P.: investigation, writing – original draft (partially).

Ponomar A.V.: investigation, resources.

Biesova O.V.: visualization, resources.

Експериментальне дослідження методу компенсації атмосферного ослаблення зондуючого лазерного випромінювання в активних оптико-електронних системах, що забезпечують підвищення контрасту зображень

Л.Ф. Купченко, А.С. Риб'як, О.А. Гурін, А.П. Гурін, А.В. Пономарь, О.В. Бєсова

Анотація. Експериментально досліджується метод компенсації атмосферного ослаблення лазерного випромінювання в активних оптико-електронних системах дистанційного зондування з динамічною обробкою оптичних сигналів для підвищення контрасту зображень. Метод компенсації атмосферного ослаблення лазерного випромінювання в активних оптико-електронних системах полягає у тому, що спектральна густина інтенсивності зондувального випромінювання формується не тільки на основі апріорних даних про спектральні характеристики відбивних поверхонь об'єкта та фону, але і з урахуванням спектрального коефіцієнта пропускання середовища, в якому поширюється оптичне випромінювання. Розроблено експериментальну установку, в якій джерелом випромінювання у передавальній частині оптико-електронної системи служать три напівпровідникові лазери, що працюють у діапазонах червоної, зеленої та синьої ділянок спектра. У ролі елементів, які імітують спектральні властивості поверхонь об'єкта і фону, що відбивають, в експерименті застосовувалися абсорбційні світлофільтри. У ролі елементів, які імітують атмосферне ослаблення, використовувалися кювети з поглинаючою оптичне випромінювання рідиною.

Ключові слова: активна оптико-електронна система, динамічна спектральна обробка, атмосферне ослаблення випромінювання, напівпровідникові лазери.